Subsampling dual-comb spectroscopy

Lukasz A. Sterczewski[1] **and Mahmood Bagheri**[1,*]

[1] *Jet Propulsion Laboratory, California Institute of Technology, Pasadena, CA 91109, USA*
[*] *Corresponding author: Mahmood.Bagheri@jpl.nasa.gov*

Published August 31, 2020 in Optics Letters Vol. 45, Issue 17. This is a preprint version of the paper.

We demonstrate a technique to compress spectral information in dual-comb spectroscopy that relies on subsampling of the electrical interferogram. It enables to reduce the data sample rate by arbitrary factors directly in the sampling process or in post-processing of existing data. Demonstration code is provided.

http://dx.doi.org/10.1364/OL.399027

Dual-comb spectroscopy (DCS) [1] has emerged as a burgeoning spectroscopic technique building upon the unique features of optical frequency combs [2]. In DCS, a pattern of sharp, narrow and equidistant optical lines carrying spectroscopic information is mapped to the radio-frequency (rf) domain via optical beating between a pair of combs with different line spacings. There is a broad demand to expand this technique into various spectral regions, as it permits broadband and high resolution measurements in extremely short time scales without any moving parts. Unfortunately, existing DCS systems are hampered by requirements on the speed of sampling electronics, which obstruct their adoption in many scenarios. It is possible, however, to relax these prerequisites by using an alternative data acquisition technique that intentionally violates the Nyquist criterion [3].

The rf comb structure of dual-comb spectra is by definition sparse, as spectroscopic information is available only at the teeth peaks separated by large gaps. This inefficient use of the electrical bandwidth becomes a significant concern for chip-scale dual-comb systems [4–7], which often produce broad multi-gigahertz-spanning rf spectra. Despite relatively few comb lines available in the spectrum with a low equivalent bandwidth, enormous amounts of data need to be acquired, stored and processed. High data throughput required for the operation of such chip-scale spectrometers may be incompatible with the vision of their battery operation and integration in portable devices. Consequently, techniques for spectral data compression and sample rate reduction become of practical relevance. This is because sampling at a slower rate typically enables use of more precise analog-to-digital converters (ADC) with higher vertical resolutions, whereas signal processing at a lower sample rate is generally more energy efficient and simplifies data-flow requirements.

Rapid progress in fast digital electronics has enabled ADCs to perform frequency translation and sampling in one operation known as IF subsampling, undersampling or direct IF-to-digital conversion. It relies on introducing controlled aliasing through sampling below the Nyquist rate, which causes the signal of interest to be replicated across the spectrum, particularly mapped to lower frequencies. In other words, we can compress a sparse broadband rf spectrum merely by using an ADC with high electrical bandwidth but operating at low sample rates.

To date, there have been presented two techniques enabling to compress rf spectra in DCS for sample rate reduction, all relying on aliasing in the optical domain. In a seminal DCS paper published in 2002 [8], Schiller proposed to double the number of lines in the electrical bandwidth without any alterations to the combs via locating the electrical beat note mapping the central part of the optical spectrum close to zero frequency. Next, in 2013 Klee et al. [9] demonstrated an alternative compression technique utilizing a pair of combs with extremely dissimilar repetition rates (i.e. with integer ratios), which was further extended by Hébert et al. [10] a year later. This scheme has proven to be useful in the characterization of semiconductor laser frequency combs using stable fiber lasers [9], however chip-scale DCS typically utilizes devices with closely matched cavities and the usefulness of this technique may be limited in such applications. To fill this niche, we propose a subsampling technique to compress spectral information in DCS relying only on sampling of the electrical beating signal below the Nyquist frequency. In other words, we introduce a technique to subsample the DCS signal obtained with a pair of closely matched combs that produces an unaliased beating spectrum on the photodetector.

Figure 1 plots an illustrative explanation of the existing and proposed spectral compression schemes. One can argue that the main difference between them lies in the location of the spectral folding axis. In Schiller's work, it is placed at zero frequency (DC), which uniformly reflects negative frequency components onto the positive frequency side along with a phase inversion. The frequency of the first rf line is simply $\Delta f_{\mathrm{rep}}/2M$, where Δf_{rep} is the repetition rate difference between the interacting combs. This scheme supports folding by a factor $M = 2$ (also known as interleaving) with two possible mapping orders: forward and reverse, as shown in Fig. 1a. It relies only on aliasing in the optical domain.

In contrast, the subsampling technique proposed here (Fig. 1b) has an arbitrary subsampling (decimation) factor M, while the main folding axis is located at $F_{S\pm}/2$ – half of the reduced sampling frequency. It inherits, however, some concepts from Schiller's work: the distance to the line closest to the (non-zero) folding axis is also $\Delta f_{\mathrm{rep}}/2M$, and the technique exploits folding around zero-frequency. What differentiates it from aliasing in the optical domain is that the compression takes place

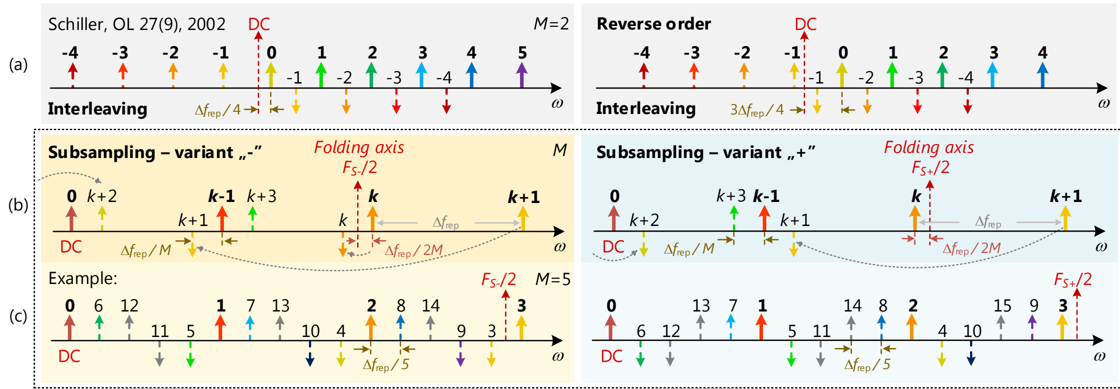

Fig. 1. Comparison between spectral folding and subsampling. (a) Spectral folding originally proposed by Schiller [8]. (b) Spectral aliasing (subsampling), which is a generalization of the folding idea. (c) Examples of subsampled spectra with $M = 5$ and $k = 3$.

during the sampling process in the ADC. Therefore, the analog bandwidths of the photodetector and ADC should ideally exceed the highest frequency of the electrical signal. In contrast, interleaving proposed by Schiller directly provides an analog electrical signal that is spectrally compressed by a factor of 2, which relaxes the analog bandwidth requirements. We will first introduce the details of our subsampling algorithm, which will be followed by a demonstration of its usefulness on real and synthetic data. The demonstration code is available in Code 1 (Ref. [11]).

Algorithm 1. Digital subsampling for DCS

Prerequisites:

1. The rf comb needs to be harmonic, i.e. the frequency of each rf line f_n is a multiple of Δf_{rep}. This condition can be easily fulfilled for virtually any offset-tunable DCS system. Because the rf offset frequency Δf_0 is defined modulo Δf_{rep}, it just needs to be tuned/locked to a multiple of it. Offset-free DCS platforms ($f_0 = 0$) like common-pump microresonators [7] are intrinsically subsampling-compatible.

2. The analog bandwidths of the detector and ADC must be higher than the highest frequency of the electrical signal.

Choice of the subsampling frequency $F_{S\pm}$:

① Calculate the order n of the highest-frequency line $f_{\max}$ in the DCS spectrum: $n = \frac{f_{\max}}{\Delta f_{\text{rep}}}$.

② Estimate the rf bandwidth occupied by a single comb line B_n and pick a subsampling factor $M \in \mathbb{N}$ such that $M \leq \lfloor \frac{\Delta f_{\text{rep}}}{B_n} \rfloor$, where $\lfloor \cdot \rfloor$ is the floor function. Due to a diversity in rf beat note powers in DCS spectra, the bandwidth definition may have to be adjusted here to a 10 dB drop in power rather than 3 dB.

③ Calculate the order of the rf comb line around which folding will occur: $k = \lceil \frac{f_{\max}}{M \cdot \Delta f_{\text{rep}}} \rceil$. $\lceil \cdot \rceil$ is the ceiling function.

④ Choose one of the two possible folding axes (frequencies) located $\frac{\Delta f_{\text{rep}}}{2M}$ away from $k\Delta f_{\text{rep}}$: $0.5F_{S\pm} = (k \pm \frac{1}{2M})\Delta f_{\text{rep}}$. Subsampling is therefore possible in two variants "+" or "-": by sampling at either F_{S+} or F_{S-} (see Fig. 1).

⑤ Validate if $n\Delta f_{\text{rep}}/M \leq F_{S\pm}/2$ to confirm that the selected $F_{S\pm}$ allows to include all lines at unique positions. If not, adjust M and repeat from step 2. If yes, sample at $F_{S\pm}$.

From a time-domain perspective, the subsampling technique requires many periods of the electrical dual-comb signal to capture an equivalent single interferogram frame. In other words, the narrower line spacing and lower sample rates are at the expense of longer acquisition times and thus lowered temporal dynamics. After subsampling, the spectrum possesses multiple comb line replicas. Of our interest is only the range $[0, F_{S\pm}/2]$. As a result of controlled aliasing, the n-th comb line appears at frequencies $f_n = |n\Delta f_{\text{rep}} + N \cdot F_{S\pm}|$, where $N = 0, \pm 1, \pm 2, \ldots$, which can be used to retrieve the new frequency axis. Deviations from the optimal (sub)sampling rate $F_{S\pm}$ introduce a slight non-uniformity in the subsampled spectrum line spacing. While in most cases it is acceptable, for large subsampling factors it may cause some of the lines to spectrally overlap. At a fixed $F_{S\pm}$, slight tuning of Δf_{rep} or a different M may be needed to ensure line equidistance.

An example application of the algorithm to synthetic dual-comb spectra is shown in Fig. 1c. The two columns show subsampling in the lower- and higher sampling frequency variant ("-" and "+") for an arbitrary factor $M = 5$. Arrows pointing downward correspond to phase inversion. The subsampling procedure in the frequency domain can be seen as a symmetric reflection (folding) around half of the new sampling frequency. After the first reflection, the neighboring (n and $n+1$) comb lines preserve their unaliased spacing Δf_{rep}, and continue to occupy new frequencies until they reach near-DC values. Around DC, a second reflection occurs and lines continue to occupy the spectrum again spaced by Δf_{rep}. This process repeats until all lines are included. The resulting spectrum has a changed order of lines but the spacing is reduced to $\Delta f_{\text{rep}}/M$ and hence the occupied bandwidth is lowered.

To better visualize that, we simulated an arbitrary spectrum consisting of 23 lines spaced by $\Delta f_{\text{rep}} \approx 23$ MHz with a linear intensity profile (Fig. 2a). It was subsampled by a factor of $M = 23$ from the original full-bandwidth signal ($F_S = MF'_{S+}$). Because of the relation between the discrete time Fourier Transform (DTFT) and the $\mathcal{Z}$-transform, we can represent the spectral magnitudes on a unit circle $|z| = 1$ as a function of a complex variable $e^{j\omega}$ with an angular frequency $\omega = \angle(e^{j\omega}) = 2\pi f$. The unit-circle representation (Fig. 2c) resembles a war bonnet with two symmetric sides. Lines in the first Nyquist zone (between angles $\omega = 0$ and half of the sampling frequency $\omega_S/2$) are unique, whereas those in the second zone between $\omega_S/2$ and ω_S are their mirrored copies. Subsampling can be envisioned as a "coiling" of the unit circle while keeping the comb teeth fixed along

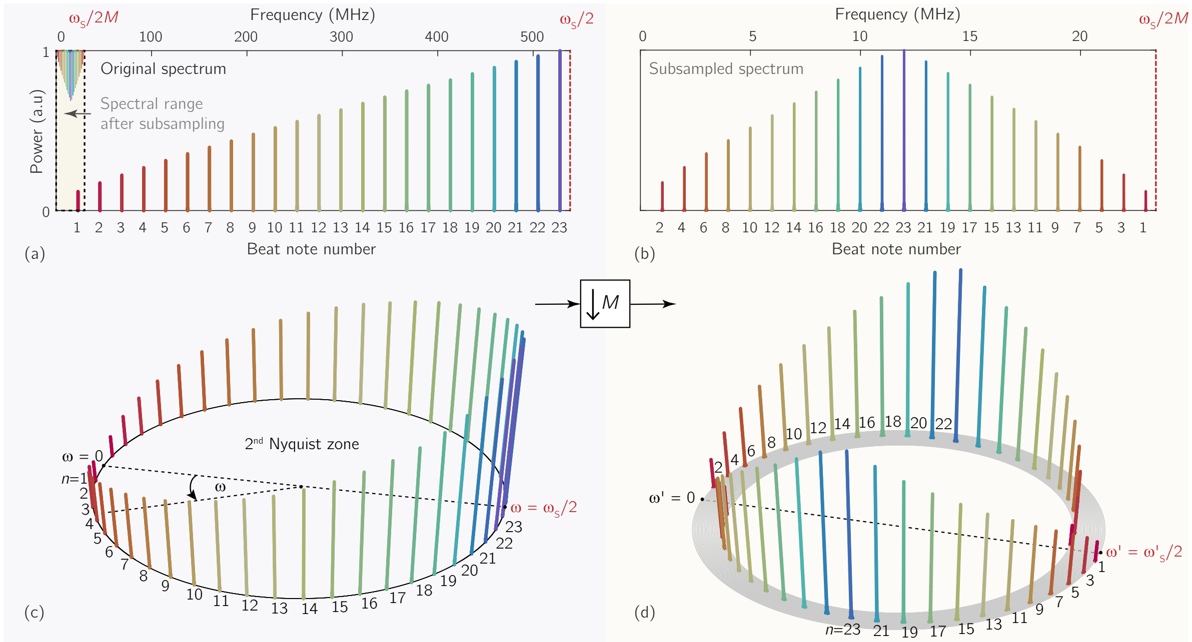

Fig. 2. Subsampling of spectra plotted in linear (a,b), and circular (c,d) representation. (a) Original non-folded spectrum plotted in the first Nyquist zone (0–$\omega_s/2$). (b) The same spectrum after subsampling with a factor of M=23. For comparison, the upper left corner of panel (a) shows the occupied bandwidth after subsampling. (c) Circular representation of the spectrum in (a) obtained by plotting the discrete time Fourier Transform (DTFT) on a unit circle. The spectrum is symmetric around the 0–$\omega_s/2$ line. (d) Subsampling viewed as wrapping the spectrum in (c) M times around the circle. In the spiral-shaped frequency axis, the turn-to-turn spacing is exaggerated to illustrate how the different comb teeth take different positions along the circle with each turn.

the circle, as shown in Fig. 2d. After subsampling, each "coil turn" introduces new comb teeth. The occupied rf bandwidth is greatly reduced (Fig. 2b) at the expense of a slight complication on the analysis side. Note that we could also set the subsampling frequency to lie below the first comb line ($F_{S-} = \Delta f_{\mathrm{rep}} - 1/M$) if $M \geq 2(n+1)$), which would correspond to ordinary compression like in normal DCS. Harmonics of F_{S-} would act as local oscillator comb lines enabling to spectrally compress the rf comb without altering its shape. In real systems, however, this scenario imposes very strict requirements on the individual comb linewidths and lower subsampling factors are preferred.

We will now demonstrate the algorithm in application to DCS data acquired from a real spectroscopic system utilizing a pair of interband cascade laser (ICL) frequency combs, as described in Ref. [12]. The sources operating around 3.6 µm had $\sim$9.7 GHz repetition rates different by $\Delta f_{\mathrm{rep}} = 22.964$ MHz. The combs were tuned via injection current to ensure that each rf comb line lies at a multiple of Δf_{rep}. In other words, the down-converted electrical signal was harmonic with no carrier-envelope offset (Δf_0). It is important to note, however, that rf comb harmonicity does not require the combs to be offset-free ($f_0 = 0$); instead only the difference in their offset frequencies (Δf_0) should vanish. In this demonstration the sources were left free running but for longer acquisitions, it is crucial to implement frequency or phase locked loops analogous to Ref. [13]. Otherwise, slight frequency drifts will cause the lines of the subsampled spectrum to overlap. Although in a real application scenario subsampling takes place directly in the ADC, for comparative purposes here we recorded the full-bandwidth signal sampled at 5 GS/s, and subsampled it in in post-processing. Fig. 3a plots the frequency spectrum covering $\sim$1.6 GHz of cumulative bandwidth. It is evident that lines on the left are broader than those on the right, which relates to Δf_{rep} (timing) fluctuations and can be accounted for using on-line adaptive clock sampling techniques [14]. For a fixed subsampling frequency $F_{S\pm}$, the compression factor must account for the widest lines, therefore we pick M=7 based on the 10-dB $B_n \approx 3.5$ MHz. The order of the highest frequency line is $n = 69$, thus $k = 10$. We pick the higher sampling frequency variant F_{S+}, which must occur at $F_{S+} = 465.84$ MHz, and results in a new subsampled repetition rate of rate of $\sim$3.28 MHz, as shown in Fig. 3b. Diversity in the beat notes' amplitudes and widths renders a slightly non-uniform spectrum but all original lines can be resolved. Stabilization of the repetition rate difference Δf_{rep} via weak injection locking [15] should address the main concern of different rf linewidths, while relative comb phase locking would allow for higher compression factors and amplitude contrast. It should be also noted that close proximity of intensive and broad rf lines may cause a significant amplitude bias of neighboring weaker lines, potentially affecting spectroscopic measurements.

This algorithm can be conveniently used to spectrally compress existing DCS data through resampling and decimation at the expense of loss in temporal resolution, which is a direct consequence of the lower Δf_{rep}. First, the existing signal must be resampled to a frequency F'_S closest to $M \cdot F_{S\pm}$, and next decimated by M. The last operation corresponds to keeping only every M-th sample, and can be performed in a phase-shifted parallel fashion known as polyphase decomposition to make use of all data points (Fig. 3c).

One of the inherent disadvantages of subsampling is aliasing of the noise, which folds from higher Nyquist zones into the first zone between 0 and $F_{S\pm}/2$. This effect causes a degradation of the spectral signal-to-noise ratio (SNR) proportional to the subsampling (decimation) factor M compared to sampling at the Nyquist rate. Therefore, in decibel scale, the noise floor

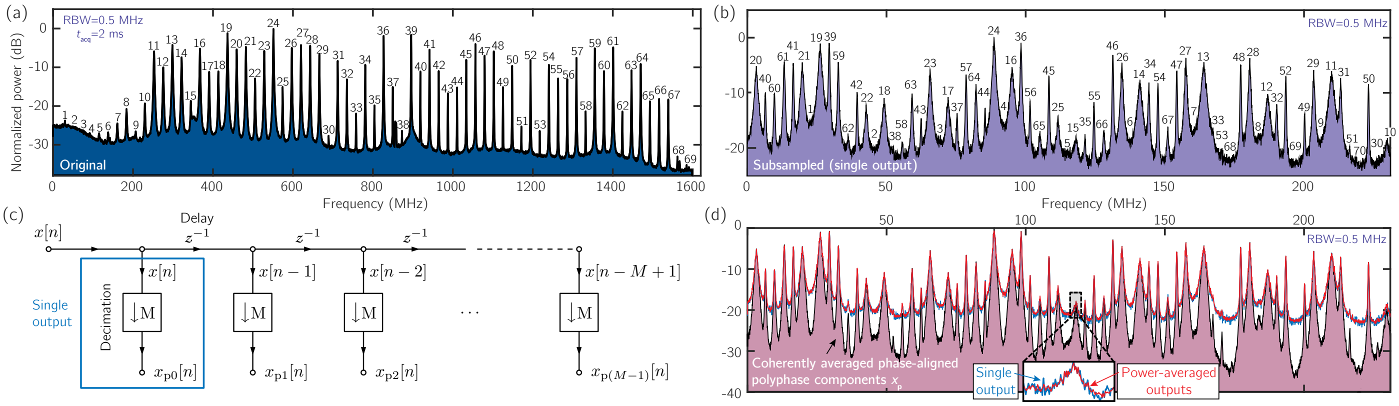

Fig. 3. Subsampling of real ICL DCS data. (a) Unaliased original spectrum. (b) Subsampled spectrum with M=7. (c) Polyphase decomposition: subsampling is realized with a sample delay. The outputs can be aligned in phase to improve the SNR. (d) Spectrum of coherently averaged x_p components compared with power (incoherent) averaging and that of a single sub-phase output as in (b).

should increase by approximately $10\log_{10}(M)$ dB, which yields 8.45 dB for $M = 7$ in agreement with the observations. To improve the SNR, samples from each polyphase output can be Fourier-transformed and averaged incoherently with a loss of phase (squared spectral magnitude averaging), or coherently with phase alignment. This operation is particularly useful for compressing existing data to suppress the influence of SNR degradation due to additive noise folding. Squared magnitude averaging, also known as video averaging allows to improve the SNR with $10\log_{10}(\sqrt{M})$ dB integration gain, but in fact it only reduces the variance of the power spectrum instead of lowering the noise floor level, as visible in the zoomed panel of Fig. 3d. The latter, can be achieved through coherent (phase aligned) averaging with $10\log_{10}(M)$ dB of gain. It should be noted that these techniques work only for additive noise, not multiplicative such as phase noise causing the rf lines to broaden.

The constant phase relationship between the polyphase outputs depends on the repetition period T_r in sample units and decimation factor M. The input signal $x[n]$ produces polyphase components $x_{\mathrm{p}d}[k] = x[(kM + d) \bmod T_\mathrm{r}]$, where $d = 0 \ldots M-1$ is the sample delay, and k is the zero-based sample index. Therefore, we need to find the minimal integer solution for $|k|$, when $x_{\mathrm{p}1}[k] = x[1]$, which corresponds to the number of polyphase samples between $x[0]$ and $x[1]$. Consequently, by comparing the indices, the equation to solve is: $(kM) \bmod T_\mathrm{r} = 1$. In our example, the repetition period T_r is $F'_S/\Delta f_\mathrm{rep} = 141$, which plugged into the equation yields a solution: $k = 141q + 121$, $q \in \mathbb{Z}$. The minimal solution $|k| = |-20|$ is for $q = -1$. A shift by $-k$ samples between the polyphase outputs applied to time-domain samples followed by their temporal (coherent) averaging improves the spectral SNR by $\sim$8 dB, as plotted in Fig. 3d. It is important to note, however, that this operation may introduce a comb filtering effect stemming from the addition of delayed versions of the sub-sampled signal. This is visible as a periodic suppression of the noise floor by more than the expected $10\log_{10}(M)$ dB, particularly in regions with weak rf lines. Fortunately, spectroscopic measurements are relative, and as long as the reference and sample spectrum are processed in the same way, this effect should not introduce severe artifacts.

In conclusion, a new approach to data compression in dual-comb spectroscopy has been proposed. Reduction of the signal sample rate with arbitrary factors is possible either by subsampling directly in the ADC or via post-processing of existing data. A possible application includes portable chip-scale spectrometers, whose battery operation necessitates lower data throughput and hence low-power consumption.

Funding. National Aeronautics and Space Agency's (NASA) PICASSO program (106822 / 811073.02.24.01.85); Universities Space Research Association (USRA), NASA Postdoctoral Program (NPP).

Acknowledgment. This work was supported under and was in part performed at the Jet Propulsion Laboratory (JPL), California Institute of Technology, under contract with the NASA. L. A. Sterczewski's research was supported by an appointment to the NASA Postdoctoral Program at JPL, administered by Universities Space Research Association under contract with NASA. The authors would like to thank Dr. Jerry Meyer, Dr. Chadwick Canedy and Dr. Igor Vurgaftman at NRL, and Dr. Clifford Frez at JPL for providing the ICL material used in this study.

Disclosures. The authors declare no conflicts of interest.

REFERENCES

1. I. Coddington, N. Newbury, and W. Swann, Optica **3**, 414 (2016).
2. N. Picqué and T. W. Hänsch, Nat. Photonics **13**, 146 (2019).
3. C. E. Shannon, Proc. IRE **37**, 10 (1949).
4. A. Dutt, C. Joshi, X. Ji, J. Cardenas, Y. Okawachi, K. Luke, A. L. Gaeta, and M. Lipson, Sci. Adv. **4**, e1701858 (2018).
5. G. Scalari, J. Faist, and N. Picqué, Appl. Phys. Lett. **114**, 150401 (2019).
6. G. Villares, A. Hugi, S. Blaser, and J. Faist, Nat. Commun. **5**, 1 (2014).
7. M. Yu, Y. Okawachi, A. G. Griffith, N. Picqué, M. Lipson, and A. L. Gaeta, Nat. communications **9**, 1 (2018).
8. S. Schiller, Opt. Lett. **27**, 766 (2002).
9. A. Klee, J. Davila-Rodriguez, C. Williams, and P. J. Delfyett, IEEE J. Sel. Top. Quantum Electron. **19**, 1100711 (2013).
10. N. B. Hébert, S. Boudreau, J. Genest, and J.-D. Deschênes, Opt. Express **22**, 29152 (2014).
11. L. A. Sterczewski, "Demonstration code for subsampling in dual-comb spectroscopy, Figshare, 2020," https://osapublishing.figshare.com/s/4cc4d69b263e1e9f8ede.
12. L. A. Sterczewski, M. Bagheri, C. Frez, C. L. Canedy, I. Vurgaftman, and J. R. Meyer, Appl. Phys. Lett. **116** (2020).
13. J. Westberg, L. Sterczewski, and G. Wysocki, Appl. Phys. Lett. **110**, 141108 (2017).
14. T. Ideguchi, A. Poisson, G. Guelachvili, N. Picqué, and T. W. Hänsch, Nat. Commun. **5**, 3375 (2014).
15. J. Hillbrand, A. M. Andrews, H. Detz, G. Strasser, and B. Schwarz, Nat. Photonics **13**, 101 (2019).